

## Removing distortions from charge balance functions

Scott Pratt\* and Sen Cheng†

*Department of Physics and Astronomy and National Superconducting Cyclotron Laboratory, Michigan State University, East Lansing, Michigan 48824, USA*

(Received 11 March 2003; published 30 July 2003)

Charge balance functions provide insight into critical issues concerning hadronization and transport in heavy-ion collisions by statistically isolating charge/anticharge pairs that are correlated by charge conservation. However, distortions from residual interactions and unbalanced charges cloud the observable. Within the context of simple models, the significance of these effects is studied by constructing balance functions in both relative rapidity and invariant relative momentum. Methods are presented for eliminating or accounting for these distortions.

DOI: 10.1103/PhysRevC.68.014907

PACS number(s): 25.75.Nq, 12.38.Mh, 25.75.Gz

### I. INTRODUCTION

Charge balance functions were suggested as a means for addressing fundamental questions concerning hadronization in relativistic heavy ion collisions [1]. The most pressing issue concerns whether hadronization is delayed in such reactions beyond the characteristic time scale of 1 fm/c, i.e., is a new phase of matter created? A delayed hadronization of a gluon-rich medium would mean that many charge-anticharge pairs would be created late in the reaction and then be more tightly correlated to one another in momentum space. Charge balance functions are designed to identify such charge-anticharge pairs on a statistical basis. Unfortunately, the ability to identify balancing partners is compromised by two effects. First, surplus charge, originating from the nonzero baryon number and charge of the colliding nuclei, pollutes the balance function. Second, interactions of a balancing pair with the other charges effectively polarize the other particles and distort the shape of the balance function. In this paper, the magnitude of such distortions is exhibited within the context of simple blast-wave models, and means for eliminating or reducing these distortions are presented.

Charge balance functions are based on conditional distributions,

$$B(P_2|P_1) \equiv \frac{1}{2} \left\{ \frac{N_{+-}(P_1, P_2) - N_{++}(P_1, P_2)}{N_+(P_1)} + \frac{N_{-+}(P_1, P_2) - N_{--}(P_1, P_2)}{N_-(P_1)} \right\}. \quad (1)$$

Here,  $N_{ab}(P_1, P_2)$  counts the incidences where a particle of charge  $a$  is observed with momentum in a region defined by  $P_1$ , while a particle of charge  $b$  is observed that satisfies the momentum constraint  $P_2$ . The second constraint could be any function of the momenta of the two particles, e.g., the relative rapidity. Put into words, the balance function measures the chance of observing an extra particle of opposite

charge, given the observation of the first particle. Balance functions are related to charge fluctuations which can be used to investigate similar issues [2–11]. The advantage of balance functions is that they represent a more differential measure.

For a neutral system, every charge has an opposite balancing charge and the balance function would integrate to unity,

$$\sum_{P_2} B(P_2|P_1) = 1. \quad (2)$$

The normalization is reduced if not all particles carrying the charge are included, e.g., only  $\pi^+$  and  $\pi^-$  are evaluated, thus neglecting the chance that the electric charge is balanced by a kaon or a baryon, or that the detector has less than a perfect acceptance. If  $P_2$  refers to the relative rapidity, and  $P_1$  includes all measured particles,  $B(P_2 = \Delta Y)$  provides the probability that a balancing charge was observed with relative rapidity  $\Delta Y$ . Since much of the charge observed in a relativistic heavy ion collision should be produced at hadronization, a delayed hadronization should result in a tighter space-time correlation between balancing charges. Due to the large collective flow fields in these reactions, a tighter correlation in space-time translates into a tighter correlation between the final momenta. Therefore, a delayed hadronization should be signaled by a narrower balance function when plotted as a function of relative momentum or relative rapidity.

One of the most enticing results from the relativistic heavy ion collider (RHIC) is the first measurement of a balance function by the STAR Collaboration [12]. In accordance with expectations for delayed hadronization, the balance functions appear to narrow with increasing centrality of the collision. However, given the nascent stage of these observations and of the phenomenology, it should be emphasized that numerous questions remain concerning the interpretation of such a measurement. To that end, several issues were pursued in a previous paper, including the effects of Hanbury Brown–Twiss correlations, detector acceptance, and the relation to charge fluctuations [2].

In the same spirit as that paper, more issues will be addressed in this study. In the following section, the benefits of analyzing balance functions in other observables, e.g., the

\*Electronic address: pratt@nscl.msu.edu

†Present address: Sloan-Swartz Center, University of California at San Francisco, 513 Parnassus Ave., Box 0444, San Francisco, CA 94143-0444.

invariant relative momentum, will be addressed. In addition to allowing one to analyze the contribution from specific resonances, it will be shown that such observables help clarify other issues such as the interplay of collective flow and cooling.

Balance function analyses are based on the assumption that all charges have balancing partners. This is not true in relativistic heavy ion collisions due to the presence of the initial protons and neutrons which bring about an imbalance of baryon number, electric charge, and isospin. In Sec. III, the distorting influence of the surplus positive charge is investigated and a modified balance function observable is proposed that would eliminate such effects.

The subsequent section contains a detailed study of the effects of interpair correlations. By extending the model presented in Ref. [2] to balance functions in  $Q_{\text{inv}}$ , it appears that the Hanbury Brown–Twiss (HBT) correlations cause a more noticeable distortion, especially in the most central collisions. The source of these residual effects is analyzed in detail, and the degree to which these distortions can be accounted for is discussed. The final section presents a summary of what further work must be done in analyzing and interpreting this class of observables.

## II. ANALYZING THE BALANCE FUNCTION IN $Q_{\text{inv}}$

In Ref. [1] balance functions were evaluated as a function of relative rapidity. Like two-particle correlation functions, the balance function is a six-dimensional quantity and new insights can be gained by performing different cuts or binnings. Specifically, we focus on performing analyses in terms of the invariant relative momentum, i.e., the relative momentum as measured by an observer moving with the velocity of the two-particle center of mass. We find that these variables yield clearer insight for interpreting the physics of the balancing charges, as well as providing a better illumination of the distorting effects which are the subject of this study.

The relative momentum of the two particles is defined,

$$\begin{aligned} q_\alpha &\equiv (p_{a,\alpha} - p_{b,\alpha}) - P_\alpha \frac{P(p_a - p_b)}{s} \\ &= (p_{a,\alpha} - p_{b,\alpha}) - P_\alpha \frac{(m_a^2 - m_b^2)}{s}. \end{aligned} \quad (3)$$

Here, the total momentum of the pair is  $P$  and the center-of-mass energy of the pair is  $\sqrt{s} = \sqrt{(p_a + p_b)^2}$ . For two particles of the same mass, the last term can be neglected. The invariant momentum is then

$$Q_{\text{inv}}^2 = -q^2 = -(p_a - p_b)^2 + \frac{(m_a^2 - m_b^2)^2}{s}. \quad (4)$$

For pion-correlation studies, it is conventional to define three projections of the relative momentum,  $Q_{\text{long}}$ ,  $Q_{\text{out}}$ , and  $Q_{\text{side}}$  [13–15]. These components measure the projections of  $q$  along the beam axis, the outwards direction (defined by the pair's transverse momentum), and the sideways direction (perpendicular to the pair's transverse momentum and to the

beam axis). Motivated by the semi-boost-invariant nature of the collision geometry at RHIC,  $Q_{\text{long}}$  is usually measured in a reference frame moving with the beam velocity of the pair. Although not typically invoked in correlations studies, one can also perform a second outwards boost to a frame where the total transverse momentum of the pair is zero. In this frame the three components,  $Q_{\text{out}}$ ,  $Q_{\text{side}}$ , and  $Q_{\text{long}}$  sum to  $Q_{\text{inv}}$ ,

$$Q_{\text{long}}^2 + Q_{\text{side}}^2 + Q_{\text{out}}^2 = Q_{\text{inv}}^2. \quad (5)$$

In terms of laboratory momenta  $P$  and  $q$ , these components are

$$\begin{aligned} Q_{\text{long}} &= \frac{1}{\sqrt{s + P_t^2}} (P_0 q_z - P_z q_0), \\ Q_{\text{side}} &= \frac{(P_x q_y - P_y q_x)}{P_t}, \\ Q_{\text{out}} &= \sqrt{\frac{s}{s + P_t^2}} \frac{(P_x q_x + P_y q_y)}{P_t}. \end{aligned} \quad (6)$$

Here,  $P_t = [(p_{a,x} + p_{b,x})^2 + (p_{a,y} + p_{b,y})^2]^{1/2}$  is the transverse momentum of the pair. These components differ from the common convention for HBT in that  $Q_{\text{out}}$  is defined as the relative momentum in the pair frame, whereas in HBT the usual convention is to ignore the second boost, which means that the three components do not sum to  $Q_{\text{inv}}$ . In fact, the factor  $\sqrt{(s + P_t^2)}/s$  in the definition of  $Q_{\text{out}}$  is simply the Lorentz gamma factor corresponding to the transverse boost to the two-particle rest frame.

Analyzing balance function in terms of  $Q_{\text{inv}}$  simplifies interpretation with thermal models by eliminating the sensitivity to collective flow. Blast-wave models are based on thermal emission from sources that move to account for the collective flow of the exploding matter. Collective flow affects the spectra, but leaves the invariant momentum differences unchanged if the two particles originate from the same space-time point of the blast wave. Hence, plotting the balance function in invariant momentum variables would minimize the confusion associated with the collective flow, as the width would only depend on the local thermal properties of the individual sources. If a particle and its balancing particle were always emitted close to one another in coordinate space, the width of the balance function would principally be a function of the breakup temperature with no sensitivity to collective flow, assuming a uniform detector acceptance.

To illustrate the complications of using rapidity differences rather than  $Q_{\text{inv}}$ , one may consider a thermal source where the width in  $Q_{\text{long}}$  is determined by the temperature. The separation of two tracks in rapidity is then,

$$\Delta y \sim \frac{Q_{\text{long}}}{m_t}, \quad (7)$$

where  $m_t$  is the transverse mass of the particles. Since collective flow affects the distribution of transverse masses, the

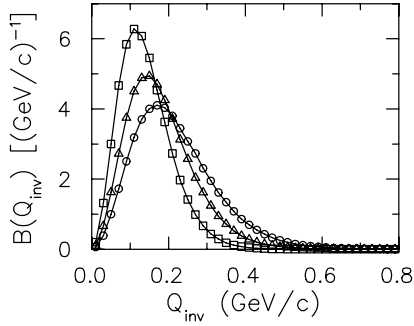


FIG. 1. Blast-wave predictions of  $\pi^+\pi^-$  balance functions are displayed for three temperatures, assuming the balancing pions are always emitted thermally from sources with identical source velocities. When plotted in  $Q_{\text{inv}}$ , the shape depends only on the breakup temperature. Calculations are shown for  $T=90$  MeV (squares),  $T=120$  MeV (triangles), and  $T=150$  MeV (circles).

balance function widths for localized thermal sources would depend on the collective flow in the data when plotted in relative rapidity. Although it is easy to account for collective flow in a theoretical model, the interpretation of experimental results is simplified by performing the analysis in  $Q_{\text{inv}}$ .

Furthermore, assuming thermal emission with highly localized charge conservation, the balance function would be isotropic with respect to the direction of the relative momentum, e.g., the width in  $Q_{\text{side}}$  would equal the width in  $Q_{\text{long}}$ . For early production of charge, one expects string dynamics or diffusion to lead to an anisotropic balance function as the balancing charges should separate significantly in coordinate space along the beam axis due to the extremely large velocity gradient along the beam axis at early times,  $dv_z/dz=1/\tau$ . Thus, in addition to the width of the balance function in  $Q_{\text{inv}}$ , the behavior of the anisotropy as a function of the collision's centrality provides a crucial test of the mechanism for charge creation and transport.

To illustrate the sensitivity of a balance function in terms of these analyses, we consider a simple blast-wave model where the collective transverse motion is assumed to rise linearly with the radius. Of the numerous parametrizations of the blast-wave model, it is assumed that the sources have transverse rapidities governed by a simple distribution,

$$\frac{dN}{y_t dy_t} = \begin{cases} \text{const.}, & y_t < \tanh^{-1}(v_{\text{max}}) \\ 0, & y_t > \tanh^{-1}(v_{\text{max}}). \end{cases} \quad (8)$$

Here,  $y_t$  is the transverse rapidity,  $\tanh(y_t)=v_{\perp}$ . The distribution of longitudinal rapidities is assumed to be uniform. For our calculation we assume that these sources emit isotropically in the source frame according to a temperature  $T$ . Balancing positive and negative pions are assumed to be emitted from sources with the same longitudinal and transverse rapidity. Figure 1 illustrates the sensitivity to the temperature by presenting balance functions for three temperatures, 90 MeV, 120 MeV, and 150 MeV. The balance function is clearly narrower for lower breakup temperatures. The results of Fig. 1 are insensitive to the choice of  $v_{\text{max}}$ . However, it must be stressed that the sensitivity would return if the balance function was analyzed in a finite acceptance.

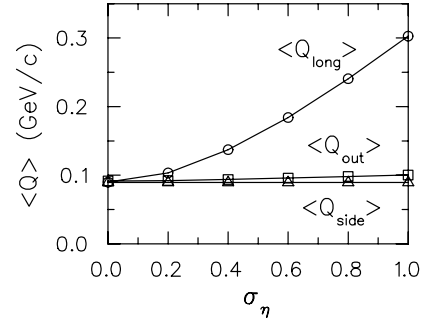


FIG. 2. The width of the balance function is shown for the three momentum components. The calculations assumed a blast-wave scenario with the collective velocities of the source points for balancing pions being separated longitudinally according to a Gaussian distribution of width  $\sigma_{\eta}$ . The calculations assumed a breakup temperature of 120 MeV and a maximum transverse collective velocity of  $0.7c$ .

The balance function could also be binned in any of the three projections,  $Q_{\text{long}}$ ,  $Q_{\text{out}}$ , and  $Q_{\text{side}}$ , rather than in  $Q_{\text{inv}}$ . If the balancing pairs were to always originate from sources with the same collective velocity, the balance function would be identical in all three variables. However, if the balancing particles were to diffuse relative to one another, the shape of the balance function might become decidedly nonisotropic. For instance, if charge is created early in a RHIC collision, the balancing charges might easily separate along the beam axis and ultimately be emitted from regions with different rapidities. Figure 2 presents the widths of balance functions, assuming that the balancing particles independently dissipated and were each ultimately emitted with sources moving with a spread of rapidities characterized by  $\sigma_{\eta}$ . A Gaussian form for the diffusion was assumed for the distribution of source rapidities,  $y_s$ ,

$$P(y_s) \sim \exp\left(-\frac{y_s^2}{2\sigma_{\eta}^2}\right). \quad (9)$$

This extends the distribution of  $Q_{\text{long}}$  while leaving the distribution of  $Q_{\text{side}}$  unaffected and the distribution of  $Q_{\text{out}}$  only slightly affected by boost effects. As can be seen in Fig. 2, the disparity in the three widths should be easily observed for this example where the temperature was chosen to be 120 MeV and the radial collective velocities were between zero and  $v_{\text{max}}=0.7c$ .

It should be difficult to discern the difference between thermal broadening and dissipation of balancing charges into regions with different collective flow. However, other observables provide insight into breakup temperature, mainly the comparison of proton and pion spectra [16]. Once one knows the breakup temperature, it is possible to fit parameters that describe the diffusive spread, e.g.,  $\sigma_{\eta}$ . Furthermore, a thermal fit to data where the diffusive terms are set to zero provides an upper bound for the breakup temperature.

For the reasons above, much of the analysis of the following sections will be given in  $Q_{\text{inv}}$ . An additional advantage of using  $Q_{\text{inv}}$  is that it allows one to identify the contribu-

tions from specific resonances which contribute peaks to the balance function when plotted in  $Q_{\text{inv}}$ . It is our hope that experimental analyses will also switch to these variables.

### III. THE EFFECTS OF SURPLUS POSITIVE CHARGE

Not all charges have balancing partners. In a Au+Au collision at RHIC, the two gold nuclei provide 158 unbalanced protons and 236 unbalanced neutrons. These pollute the balance function by providing unbalanced electric charge, baryon number, and isospin. For detectors like STAR, these effects are lessened by the fact that most of the surplus charge is at high rapidity and outside the experimental acceptance. However, the effect should become more significant if the balance function is constructed for a set of charges, e.g.,  $p\bar{p}$ , for which there is a significant imbalance of one charge versus the opposite charge. Our goal in this section is to offer a revised procedure for producing balance functions from data that would subtract the pollution due to the surplus charge. More precisely, we wish to define a balance function that would ignore any additional unbalanced charges that are not correlated with one another or with pairwise created charges.

In order to demonstrate the effects of the polluting surplus charge, we introduce a notation where distributions  $\bar{N}$  count charges that are divided into three categories. The subscripts “+” and “-” will refer to positive and negative charges that are created in tandem. The subscripts “ $\delta$ ” will denote the surplus positive charge. The balance function will be re-evaluated after inserting the replacements,

$$\begin{aligned}
N_- &\rightarrow \bar{N}_-, \\
N_+ &\rightarrow \bar{N}_+ + \bar{N}_\delta, \\
N_{--} &\rightarrow \bar{N}_{--}, \\
N_{++} &\rightarrow \bar{N}_{++} + \bar{N}_{\delta+} + \bar{N}_{+\delta} + \bar{N}_{\delta\delta}, \\
N_{+-} &\rightarrow \bar{N}_{+-} + \bar{N}_{\delta-}, \\
N_{-+} &\rightarrow \bar{N}_{-+} + \bar{N}_{-\delta},
\end{aligned} \tag{10}$$

into Eq. (1),

$$\begin{aligned}
B(P_2|P_1) &= \frac{[2\bar{N}_+(P_1) + \bar{N}_\delta(P_1)]}{2[\bar{N}_+(P_1) + \bar{N}_\delta(P_1)]} \\
&\cdot \frac{\bar{N}_{+-}(P_1, P_2) - \bar{N}_{++}(P_1, P_2)}{\bar{N}_+(P_1)} \\
&+ \frac{\bar{N}_\delta(P_1)\bar{N}_{+\delta}(P_1, P_2) - \bar{N}_+(P_1)\bar{N}_{\delta\delta}(P_1, P_2)}{2[\bar{N}_+(P_1) + \bar{N}_\delta(P_1)]\bar{N}_+(P_1)}. \tag{11}
\end{aligned}$$

In deriving Eq. (11) an explicit symmetry between the positive and negative charges has been assumed, i.e.,  $\bar{N}_+ = \bar{N}_-$ ,

$\bar{N}_{++} = \bar{N}_{--}$ , and  $\bar{N}_{+-} = \bar{N}_{-+}$ . The first term in this expression is proportional to the unpolluted balance function  $\bar{B}$ . The second term can be simplified by assuming that the surplus charges are uncorrelated with the other charges and that they are also uncorrelated with themselves, aside from overall conservation of charge,

$$\bar{N}_+(P_1)\bar{N}_{\delta\delta}(P_1, P_2) = \bar{N}_\delta(P_1)\bar{N}_{\delta+}(P_1, P_2)\frac{Q-1}{Q}, \tag{12}$$

where  $Q$  represents the maximum integrated surplus charge. The balance function can then be expressed as

$$\begin{aligned}
B(P_2|P_1) &= \frac{[2\bar{N}_+(P_1) + \bar{N}_\delta(P_1)]}{2[\bar{N}_+(P_1) + \bar{N}_\delta(P_1)]}\bar{B}(P_2|P_1) \\
&+ \frac{1}{Q-1} \cdot \frac{\bar{N}_{\delta\delta}(P_1, P_2)}{2[\bar{N}_+(P_1) + \bar{N}_\delta(P_1)]}, \\
\bar{B}(P_2|P_1) &\equiv \frac{\bar{N}_{+-}(P_1, P_2) - \bar{N}_{++}(P_1, P_2)}{\bar{N}_+(P_1)}. \tag{13}
\end{aligned}$$

If the charges used to construct the balance function obey strict charge conservation, a perfect detector would satisfy the normalization conditions,

$$\begin{aligned}
\sum_{P_2} \bar{B}(P_2|P_1) &= 1, \\
\sum_{P_2} \bar{N}_\delta(P_2) &= Q, \\
\sum_{P_2} \bar{N}_{\delta\delta}(P_1, P_2) &= \bar{N}_\delta(P_1)\frac{Q-1}{Q}. \tag{14}
\end{aligned}$$

After inserting Eq. (14) into Eq. (13), one can see that the normalization of the balance function is unchanged by the surplus charge. However, the shape is altered as the balance function comprises two components. The first term in Eq. (13) describes the separation of balancing charges, while the second term is governed by the separation of two random balancing charges. The relative weight of the two terms is determined by the fraction of the charge owes itself to a surplus in the initial state. Thus, the effect of the surplus charge is to dampen the contribution from the balancing charges and to average in a second contribution.

For the STAR detector at RHIC, this second term is fairly small even for protons as the number of surplus protons is less than 10 per unit rapidity in central collisions [17]. Given that charge conservation constraints would suggest  $Q = 158$ , the effect of the extra charge is to first dampen the balance function by approximately 15%, and second to add in a second component whose width is characteristic of the acceptance, and whose magnitude is only 1% or 2% of the contribution from balancing charges.

In order to eliminate the contribution from surplus charge and determine  $\bar{B}$  from experiment, one can consider an object similar as to what is used to create the balance function numerator using mixed events. This object will be referred to as  $M(P_1, P_2)$  and will be constructed from mixed events, where  $N_{a,b}^m(P_1, P_2)$  signifies that the charges  $a$  and  $b$  which satisfy the momentum constraints  $P_1$  and  $P_2$  are chosen from separate events,

$$\begin{aligned} M(P_1, P_2) &\equiv N_{+-}^m(P_1, P_2) - N_{++}^m(P_1, P_2) + N_{-+}^m(P_1, P_2) \\ &\quad - N_{--}^m(P_1, P_2) \\ &= \bar{N}_{+-}^m(P_1, P_2) - \bar{N}_{++}^m(P_1, P_2) \\ &\quad + \bar{N}_{-+}^m(P_1, P_2) - \bar{N}_{--}^m(P_1, P_2), \\ &- \bar{N}_{+\delta}^m(P_1, P_2) - \bar{N}_{\delta+}^m(P_1, P_2) - \bar{N}_{\delta\delta}^m(P_1, P_2) + \bar{N}_{-\delta}^m(P_1, P_2) \\ &+ \bar{N}_{\delta-}^m(P_1, P_2). \end{aligned} \quad (15)$$

Since the counts for different events are independent,  $N_{+-}^m = N_{++}^m = N_{-+}^m = N_{--}^m$ ,  $N_{\delta+}^m = N_{\delta-}^m$  and  $N_{+\delta}^m = N_{-\delta}^m$ . Thus,  $M$  becomes

$$M(P_1, P_2) = -\bar{N}_{\delta\delta}^m(P_1, P_2). \quad (16)$$

One could define a similar object using pairs from the same event,

$$\begin{aligned} N(P_1, P_2) &\equiv N_{+-}(P_1, P_2) - N_{++}(P_1, P_2) \\ &\quad + N_{-+}(P_1, P_2) - N_{--}(P_1, P_2) \\ &= \bar{N}_{+-}(P_1, P_2) - \bar{N}_{++}(P_1, P_2) \\ &\quad + \bar{N}_{-+}(P_1, P_2) - \bar{N}_{--}(P_1, P_2) - \bar{N}_{\delta\delta}(P_1, P_2). \end{aligned} \quad (17)$$

Again if one assumes that the only correlation between surplus charges involves a constraint on the overall number of surplus charges,

$$\begin{aligned} N(P_1, P_2) &= \bar{N}_{+-}(P_1, P_2) - \bar{N}_{++}(P_1, P_2) + \bar{N}_{-+}(P_1, P_2) \\ &\quad - \bar{N}_{--}(P_1, P_2) - \frac{Q-1}{Q} \bar{N}_{\delta\delta}^m(P_1, P_2). \end{aligned} \quad (18)$$

One can then generate the desired balance function  $\bar{B}(P_2|P_1)$  by combining  $N$  and  $M$ ,

$$\bar{B}(P_2|P_1) = \frac{N(P_1, P_2) - M(P_1, P_2)(Q-1)/Q}{N_{<}(P_1)}, \quad (19)$$

where  $N_{<}$  is  $N_-$  if the surplus charges are positive and is  $N_+$  if the surplus charges are negative.

It should be emphasized that this derivation assumed that the detector has equal acceptance for positive and negative charges. The ability of  $\bar{B}$  to ignore the polluting surplus charge is based on the assumption that the surplus charges

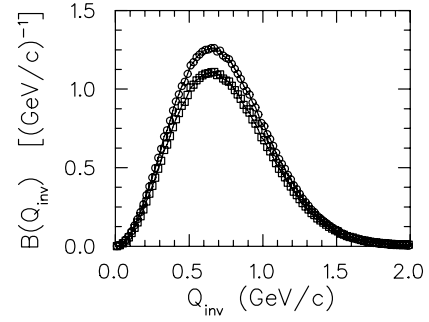


FIG. 3. Proton-antiproton balance functions are shown for a blast-wave model with and without corrections for the surplus unbalanced protons. The corrected balance function (circles) is constructed assuming a breakup temperature of 120 MeV, a maximum transverse velocity of  $0.7c$ , and  $\sigma_\eta = 0$ . The calculation was scaled down by 40% to account for balancing of the proton's charges by other species. The distorted balance function (squares) is based on the proton excess, as measured by the BRAHMS Collaboration. Both balance functions were filtered through the STAR acceptance.

are uncorrelated with one another and are equally correlated with the “+” and “-” charges. As discussed in the following section and in Ref. [2], such correlations can be important, especially at small relative momentum.

To illustrate the importance of these corrections, we generate a  $p\bar{p}$  balance function from a simple model of a boost-invariant emission of particles governed by a temperature of 120 MeV and a maximum transverse velocity of  $0.7c$ . It is assumed that the number of protons per unit rapidity is 28 and that the number of antiprotons is 21, to be consistent with measurements from RHIC [17]. The polluted balance function as described in Eq. (13) is displayed in Fig. 3 along with the corrected balance function  $\bar{B}$ . This calculation is generated by assuming that particles were emitted from sources with random rapidities, but that two balancing particles are emitted from sources with the same velocity. The parameter  $Q$  used in Eq. (13) is assumed to be 158.

Two additional modifications have been added to Eq. (13) in order to more fairly illustrate the magnitude of the effect of the surplus charge. First, the function  $\bar{B}$  was scaled down by 40% to account for the fact that the charge of an antiproton is often balanced by a neutron or by a  $\Lambda$ . Second, the simulated momenta were put through an acceptance filter that crudely mocks the acceptance of the STAR detector at RHIC. Particles were required to have a  $p_t$  greater than 100 MeV/c and a momentum of magnitude less than 700 MeV/c. The pseudorapidities were confined to a region of midrapidity,  $-1.1 < \eta < 1.1$ .

As illustrated in Fig. 3, the effects of the extra charge are mainly to dampen the balance function. The importance of correcting for the surplus charge would certainly be magnified if one were to analyze balance functions from SPS or AGS collisions where the fraction of extra protons is much higher. These corrections are not model dependent, and the corrected balance functions exactly reproduce  $\bar{B}$ . However, it should be emphasized that this statement relies on the as-

sumption that the surplus charge is uncorrelated with other surplus charges, and with the pairwise created charges.

#### IV. FINAL-STATE INTERACTION DISTORTION TO THE BALANCE FUNCTION

The balance function is implicitly predicated on the assumption that there are no residual correlations between a given charge and all other charges besides its balancing partner, i.e., all other charges are statistically eliminated from the distribution by the like-sign subtraction. Not all correlations cause problems. For instance, flow correlations tend to be identical between particles of the opposite charge or the same charge and thus fall out of the balance function. On the other hand, final-state interactions involve all the other charges and depend sensitively on the relative signs of the charges. This distortion can rise linearly with the multiplicity since the number of charges with which a given charge can correlate rises linearly with the multiplicity. However, correlation functions tend to approach unity at higher multiplicity in accordance with expectations for increasing source size. This makes the resulting multiplicity dependence of the distortion nontrivial.

A method for estimating the distortion to the balance function from residual interactions was provided in Ref. [2]. The same method is applied here. For every balancing pair,  $p_a$  and  $p_b$ , one must consider the correlation weight with other pairs whose momenta are  $p_c$  and  $p_d$ . The weight  $w(p_a, p_b; p_c, p_d)$  can be estimated,

$$w(p_a, p_b; p_c, p_d) \approx C_{++}(p_a, p_c) C_{--}(p_b, p_d) C_{+-}(p_a, p_d) C_{-+}(p_b, p_c). \quad (20)$$

Ideally, the balance function would isolate the  $ab$  pair and the interaction with the  $cd$  pair would cancel from the subtraction,  $N_{+-} - N_{++}$ . The correlations will lead to distortions if

$$w(p_a, p_b; p_c, p_d) \neq w(p_a, p_b; p_d, p_c). \quad (21)$$

That is, distortions are caused only by those interactions that differ between same-sign and opposite-sign particles. For instance, an isoscalar exchange between pions would not bring on a distortion, but a Coulomb interaction or identical-particle interference would provide a source for distortion.

We simulate these effects for  $\pi^+ \pi^-$  balance functions with the same blast-wave model described in Sec. II. The source of the  $ab$  pairs was chosen to move with one randomly chosen velocity, while the  $cd$  source was chosen to move with a different velocity. The distributions were calculated for the balance function numerators using the four particles, but rather than incrementing the distributions by unity, the distributions were incremented by the weight described in Eq. (20). The correlation functions used to calculate the weights were generated by the form

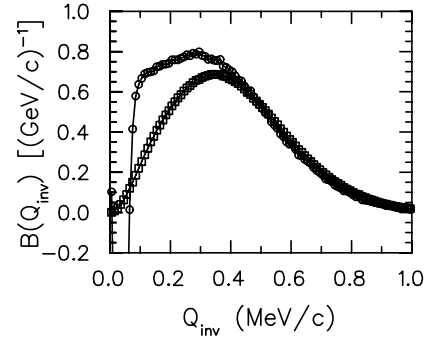


FIG. 4. As a function of  $Q_{inv}$ ,  $\pi^+ \pi^-$  balance functions from a blast-wave model are shown with (circles) and without (squares) the distorting effects of interpair interactions. The model assumed a breakup temperature of 120 MeV, a maximum transverse velocity of  $0.7c$ , and  $\sigma_{\eta} = 0$ . The undistorted balance function was scaled by 70% to account for balancing by other species, and both balance functions were filtered by the STAR acceptance. The significant enhancement for momenta between 60 MeV/c and 400 MeV/c owes itself to the Coulomb interaction between pions.

$$C(p_a, p_b) = \int d^3r g(\mathbf{r}) |\phi(\mathbf{q}, \mathbf{r})|^2, \quad (22)$$

where  $\mathbf{q}$  is the relative momentum in the two-pion frame. The wave functions  $\phi(\mathbf{q}, \mathbf{r})$  are simply symmetrized Coulomb waves with no correction for the strong interaction. The source function  $g(\mathbf{r})$  is a Gaussian source of radius  $R_{inv} = 6.0$  fm, consistent with measurements at RHIC [19]. A more sophisticated treatment would account for the  $p_t$  dependence and the sensitivity to the direction of the relative momentum. The distortion is proportional to the multiplicity of charged pions, which was chosen to be 300 for both positive and negative pions, again roughly consistent with measurements at RHIC [18].

By considering the contributions due to the extra weight separately from the usual contributions arising between the balancing particles, and weighting them appropriately for the given value of  $dn/dy$ , balance functions were calculated with and without the effects of residual interactions. Results are shown in Figs. 4 and 5. A crude filter for the STAR detector at RHIC was applied and it was assumed that 70%

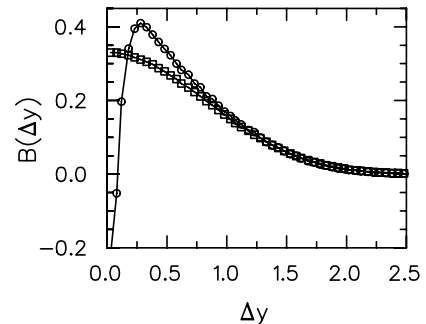


FIG. 5. The same as Fig. 4, only with the balance function being plotted as a function of relative rapidity. The distorting effects are less noticeable in  $\Delta y$ .

of the pions had their charge balanced by other pions, which affects the normalization of the balance function.

Residual interactions can either strengthen or diminish the balance function depending on the relative momentum. At very small relative momentum, the balance function at small relative momentum rises due to the Coulomb enhancement of the  $\pi^+\pi^-$  correlation function and the Coulomb repulsion of the  $\pi^+\pi^+$  and  $\pi^-\pi^-$  correlation functions. For values of  $Q_{\text{inv}}$  larger than a few MeV/c but less than  $\sim 25$  MeV/c, the identical-particle interference that enhances the  $\pi^+\pi^+$  and  $\pi^-\pi^-$  correlation functions, diminishes the balance function since same-sign pairs contribute negatively to the balance function. At larger relative momenta, Coulomb effects again dominate. The effects are less dramatic when the balance function is viewed as a function of relative rapidity.

The distortion of the balance function in Fig. 4 is dominated by Coulomb effects at large momentum. The correlation weights are driven by the squared quantum wave function. However, the correlation for large values of  $qR$  can be understood by considering the classical analog to the wave function. As shown in Ref. [20], the classical analog is

$$\begin{aligned} |\phi(q,r)|^2 &\rightarrow \frac{d^3q_i}{d^3q_f} = \frac{q_i}{q_f} \\ &= \sqrt{1 - 8Z_a Z_b \alpha \mu / r q_f^2} \\ &\approx 1 - 4Z_a Z_b \alpha \mu / r q_f^2, \end{aligned} \quad (23)$$

where  $\alpha$  is the fine structure constant, the product of the charges of the two species is  $Z_a Z_b$ ,  $\mu$  is the reduced mass, and  $q_i$  and  $q_f = Q_{\text{inv}}$  are the initial and final relative momenta. Thus, the effects of Coulomb interactions, in the classical limit, only diminish as a function of  $1/Q_{\text{inv}}^2$ . By averaging  $1/r$  over a Gaussian source characterized by the Gaussian source size  $R$ , one can find the asymptotic form for the classical correlation function,

$$C_{\text{class}}(Q_{\text{inv}}) \approx 1 - \frac{4\mu\alpha Z_a Z_b}{Q_{\text{inv}}^2 R \sqrt{\pi}}. \quad (24)$$

The classical result for the  $\pi^+\pi^-$  correlation function is compared to the quantum result for a 6-fm source in Fig. 6. The agreement is remarkable for  $Q_{\text{inv}} > 25$  MeV/c when  $qR > 1$ , especially for the opposite-sign case where there is no identical-particle interference.

Even though the correlation function goes to zero proportional to  $1/Q_{\text{inv}}^2$ , the phase space is increasing as  $Q_{\text{inv}}^2$ . Thus, the Coulomb interaction remains important to remarkably large momenta. For more central collisions, the value of  $R$  rises, but the number of particles with which a given particle is correlated also rises. If the multiplicity scales as  $R^3$ , it is clear that the Coulomb distortion will become acute for central collisions.

Strong-interaction distortions have not been considered in these calculations. In terms of the  $\pi\pi$  phase shifts  $\delta_\ell$ , the contribution to the correlation function from strong interactions can be approximated by the relation [21]

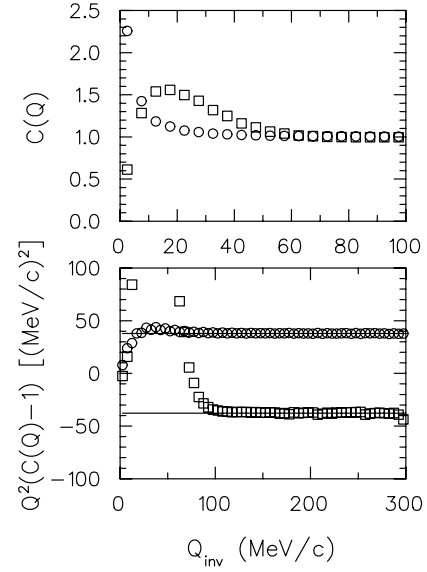


FIG. 6. Correlations for same-sign (squares) and opposite-sign (circles) pions are shown for a Gaussian source of size  $R=6$  fm in the upper panel. To illustrate the Coulomb effects that force  $C(Q)$  to approach unity as  $1/Q^2$ ,  $C(Q)-1$  is multiplied by  $Q^2$  and displayed in the lower panel. The lines represent the constant expected for Coulomb interactions described in Eq. (24). Since phase space increases as  $Q^2$ , interpair correlations distort the balance functions for relative momenta of several hundred MeV/c.

$$C(q) \sim \frac{1}{4q^2 R^3 \sqrt{\pi}} (2\ell + 1) \frac{d\delta_\ell}{dq}. \quad (25)$$

The strength of the strong-interaction correlation falls much more quickly with  $R$  than does Coulomb-induced correlation. If  $R^3$  were to scale linearly with multiplicity, the effect of the strong interaction on the balance function would be roughly independent of multiplicity or centrality. This difference in the behavior derives from the fact that a given pion interacts with only its neighbors through the strong interaction, while it may interact with nearly all particles through the Coulomb interaction. If the breakup density is independent of centrality, the number of neighbors stays constant and the distortion to the balance function from strong interactions should not be strongly centrality dependent. On the other hand, the Coulomb distortion interaction should be much stronger for central collisions than for peripheral collisions.

The ingredients for calculating the distortion were the correlation weights and spectra along with the procedure for generating the pairs,  $(p_a, p_b)$  and  $(p_c, p_d)$ . In principal, the spectra and correlation weights can be taken or inferred from data without introducing a theoretical model. However, the generation of the pairs cannot be extracted directly from data due to the correlations between  $p_a$  and  $p_b$  and those between  $p_c$  and  $p_d$ . Since particles are produced pairwise, it is necessary to include these correlations because the interpair interaction must attract pairs rather than single particles. That is, the net charge in the medium cannot change, but it can be polarized. At face value, this is an explicit model dependence. However, the parameters that govern the correlation

between  $a$  and  $b$  and between  $c$  and  $d$  are precisely those parameters used to model the undistorted balance function. Thus, no additional model parameters would be introduced to calculate the distortion. Thus, the distortion from residual interactions cannot be subtracted from experimental results in a model-independent fashion, but it can be modeled theoretically without additional parameters.

Given the significant effects from interpair correlations, it is imperative that the balance function analyses correct for these distortions. Fortunately, the corrections can be confidently modeled, and the robustness of the balance function is not compromised. However, this conclusion is predicated on an understanding of the two-particle correlations. Since a correlation of a fraction of a percent can significantly alter the balance function, the issue of strong-interaction corrections to the balance functions should be revisited.

Strong-interaction effects can be divided into two categories. The first category would be  $s$ -channel interaction that has particle-antiparticle channels, e.g.,  $\rho^0 \rightarrow \pi^+ \pi^-$ . But, this source should not be considered as a distortion since the two pions are indeed a balancing pair. For instance, if all pions resulted from  $\rho^0$  decays, the balance function would peak at the invariant mass of the  $\rho$ , and provide an important clue as to the creation mechanism for pions. Such resonant contributions can be calculated in a microscopic model or in a thermal calculation based on the canonical ensemble. A second source of strong-interaction effects is the interaction with other bodies through nonresonant interactions. Since the strong interaction is short range, this interaction should involve only a few neighbors. For large sources, the Coulomb interaction provides a larger effect on two-particle correlation function than does the strong interaction. Nonetheless, it would be worthwhile to better quantify the significance or insignificance of the strong interaction.

## V. SUMMARY AND DISCUSSION

Charge balance functions were developed with the hope of identifying balancing charges on a statistical basis. Two effects prevent the like-sign subtraction from accomplishing this goal to high precision. As shown in Sec. III, the excess nucleons coming from the colliding nuclei provide a modest pollution to the balance function in measurements at mid-rapidity at RHIC. Fortunately, these effects can be easily subtracted. The second source of distortion derives from the interpair interaction of balancing charges with other particles in the medium. These distortions become more important in high multiplicity events. As shown in Sec. IV, for high multiplicity events these distortions are most strongly affected by the Coulomb interaction. These effects are also more noticeable for balance functions calculated in  $Q_{\text{inv}}$  than they are for balance functions calculated in relative rapidity. Although it is difficult to subtract these distortions in a model-independent fashion, it is straightforward to include these effects in a theoretical treatment. In addition to the typical parameters one would use to model balance functions, modeling the distortion requires only an additional understanding of two-particle correlations. As these correlations can be extracted from measurement, the distortion from interpair interactions can be modeled quite confidently. In central collisions, this distortion can be a 20% effect, and if the correlation functions are understood to the 90% level, the residual systematic uncertainty is probably of the order of 1% or 2%.

## ACKNOWLEDGMENTS

This work was supported by the National Science Foundation, Grant No. PHY-00-70818.

- 
- [1] S.A. Bass, P. Danielewicz, and S. Pratt, Phys. Rev. Lett. **85**, 2689 (2000).
  - [2] S. Jeon and S. Pratt, Phys. Rev. C **65**, 044902 (2002).
  - [3] M. Asakawa, U. Heinz, and B. Muller, Phys. Rev. Lett. **85**, 2072 (2000).
  - [4] M. Asakawa, U.W. Heinz, and B. Muller, Nucl. Phys. **A698**, 519 (2002).
  - [5] V. Koch, Acta Phys. Pol. B **33**, 4219 (2002).
  - [6] V. Koch, M. Bleicher, and S. Jeon, Nucl. Phys. **A698**, 261 (2002).
  - [7] M. Bleicher, S. Jeon, and V. Koch, Phys. Rev. C **62**, 061902(R) (2000).
  - [8] S. Jeon and V. Koch, Phys. Rev. Lett. **85**, 2076 (2000).
  - [9] M. Abdel-Aziz and S. Gavin, Nucl. Phys. (to be published).
  - [10] C. Pruneau, S. Gavin, and S. Voloshin, Phys. Rev. C **66**, 044904 (2002).
  - [11] S. Gavin and J.I. Kapusta, Phys. Rev. C **65**, 054910 (2002).
  - [12] J. Adams *et al.*, Phys. Rev. Lett. **90**, 172301 (2003).
  - [13] S. Pratt, Phys. Rev. D **33**, 1314 (1986).
  - [14] G.F. Bertsch, Nucl. Phys. **A498**, 173c (1989).
  - [15] T. Csörgő, J. Zimányi, J. Bondorf, H. Heiselberg, and S. Pratt, Phys. Lett. **B241**, 301 (1990).
  - [16] K. Adcox *et al.*, Phys. Rev. Lett. **88**, 242301 (2002).
  - [17] J.H. Lee, BRAHMS Collaboration, Nucl. Phys. (to be published).
  - [18] T. Chujo, PHENIX Collaboration, Nucl. Phys. (to be published).
  - [19] C. Adler *et al.*, Phys. Rev. Lett. **87**, 082301 (2001).
  - [20] Y.D. Kim, R.T. de Souza, C.K. Gelbke, W.C. Gong, and S. Pratt, Phys. Rev. C **45**, 387 (1992).
  - [21] B.K. Jennings, D.H. Boal, and J.C. Shillcock, Phys. Rev. C **33**, 1303 (1986).